

Earthquake Geotechnics in Offshore Engineering

Amir M. Kaynia

Norwegian Geotechnical Institute (NGI), Oslo, Norway, amir.m.kaynia@ngi.no
Norwegian University of Science and Technology (NTNU), Trondheim, Norway

Abstract This paper presents a number of geotechnical issues encountered in earthquake design of offshore structures and subsea facilities. Parallel with construction of traditional structures such as jackets and gravity-based structures, a considerable effort has recently been put to field developments in deep water. This has brought about other challenges that are largely dependent on geotechnical knowledge. This paper addresses some of the more recent approaches and solutions in geotechnical earthquake design of both shallow water and deep-water structures and facilities such as platforms with large bases, pipelines traversing slopes and seabed installations. It is demonstrated how incorporation of radiation damping and nonlinear soil-structure interaction in offshore installations could optimize the design. Considering the importance of earthquake stability of slopes in deep water development, special attention is given to highlighting several key issues in the earthquake response of submarine slopes including strain softening and three-dimensional shaking.

1. Introduction

This paper addresses a number of key geotechnical issues encountered in earthquake design of offshore structures and subsea facilities. The topics include fixed offshore platforms, including jacketed and gravity-based structures, earthquake analysis and stability of submarine slopes, response of pipelines, and subsea facilities. For offshore wind turbines, the reader is referred to other publications (e.g. Kaynia, 2017). The main geotechnical issue in the earthquake analysis of jacketed offshore platforms is design of piles. Use of analytical solution and empirical methods based on p-y concept are discussed, and the effect of liquefaction on pile analysis is reviewed. In gravity-based structures, the main issue is analysis of soil-structure interaction

(SSI). To this end, the existing solutions for SSI analyses are reviewed and extension of the conventional three-step method to cases with flexible bases and nonlinear response are discussed.

With recent trends in deep water oil and gas development, the earthquake response of submarine slope has become a major issue. In this connection, the role of several factors such as strain softening, multi-direction earthquake shaking and 3-D slope geometry on earthquake response of slopes are evaluated by numerical solutions. Moreover, the response of pipelines traversing slopes are investigated using a numerical model developed for this purpose. Finally, the earthquake response of seabed facilities, such as manifolds are presented and the critical role of radiation damping in reducing the earthquake loading is demonstrated.

2. Seismic Design Philosophy

The seismic design philosophy in offshore design generally follows ISO standards for offshore structures. They require achieving acceptable low risks with respect to Health, Safety, and the Environment (HSE), economic loss, and interruption to normal operations (Younan et al. 2015). This design philosophy is reflected in the following two performance expectations:

1. Little or no damage or interruptions to normal operations during frequent earthquakes referred to as Extreme Level Earthquake (ELE) with return periods typically in the range 300-700 years.
2. No serious HSE consequences in rare earthquakes referred to as Abnormal Level Earthquake (ALE) with typical return periods in the range 2500-4000 years although the facility could be irreparable and result in an economic loss.

ISO 19901-2 (2004) has established a procedure for determination of the design return periods based on the seismic hazard condition at the site and ductility performance of the structures. In addition to these events, some operators demand demonstration of sufficient residual capacity to survive nominal post-ALE events, including aftershocks, to allow safe shutdown of facilities and rescue of personnel (Younan et al., 2015).

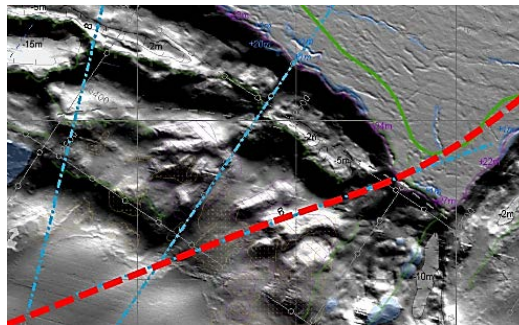
The input to earthquake analyses consists of time-history records, often representing bedrock or stiff soil outcrop, and matched to a uniform hazard spectrum (UHS) established by a probabilistic seismic hazard analysis (PSHA) covering both ELE and ALE events.

3. Earthquake Response of Submarine Slopes

Slopes are often encountered in the development of offshore fields in deep water. Even in cases where the seabed is flat at the location of the platforms and wells,

there is often a need to connect a series of subsea clusters, or transport the oil and gas by pipeline to a near offshore platform or an onshore processing and storage facility. In such cases, the pipelines often have to cross or traverse slopes. Large downslope movement in slopes under earthquake can potentially damage the pipeline, and in the event of landslide, the moving failed mass can impact and destroy the subsea facilities located downstream from the escarpment. Figure 1 shows an example of a deep-water site in which pipelines are considered to run upslope in order to connect to the platform.

Fig. 1. Pipeline (dashed line) traversing submarine slope displaying earlier landslides

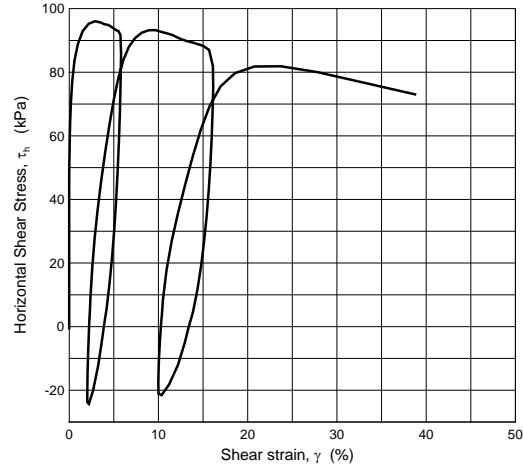


A variety of codes are available for numerical simulation of slope response under earthquake loading. The codes include 1-D solutions, 2-D models (e.g. PLAXIS and FLAC) and 3-D tools (e.g. PLAXIS 3D and FLAC3D). Analyses of slopes are therefore standardized in practice. This section addresses issues either not covered by these codes or ignored in practice often due to their complexity. They include: a) strain softening, b) multi-directional shaking, and c) three-dimensional geometry.

3.1 Strain Softening

Geophysical surveys and geotechnical investigations at several deep offshore sites have indicated landslides in slopes with even small angles. Some of the compelling arguments for triggering of these landslides are reduction of the soil's shear strength due to strain softening under cyclic earthquake loading, post-earthquake failure due to creep (e.g. Nadim et al. 2006; Andersen, 2009), and/or significant reduction of the static shear strength post cyclic loading. The latter subject is addressed in the next section. The strain softening behavior is illustrated in Fig. 2 by the stress-strain diagram for a DSS test on a clay sample from an offshore site. The intention was to run the test at constant stress, but the early failure of the sample helped capture the strain-softening response of the soil during subsequent cycles. A series of centrifuge dynamic tests have recently been carried out by Park and Kutter (2015) on sensitive clay. The results will provide a valuable opportunity to understand the dynamic behavior of sensitive clays and to calibrate or verify the existing numerical models.

Fig. 2. Stress-strain curve for direct simple shear, DSS, test on sensitive clay



To assess the effect of strain softening numerically, a number of 1-D analyses were performed using the numerical code *QUIVER_slope* (Kaynia, 2012a). To this end, the software was first validated against a commercial 2D code for elastic-perfectly plastic (Mohr-Coulomb) soil behavior. An earthquake excitation with PGA = 0.3 g was applied at bedrock at 100 m depth. The top 50 m of the soil is NC clay with the normalized static shear strength $s_u^{DSS} = 0.20\sigma_v'$ and $G_{max}/s_u^{DSS} = 1100$. To account for the rate effect, the peak shear strength was increased by 30%. The value of G_{max} in the elastic layer (from 50 m depth) was taken equal to 132 MPa, which is 50% larger than G_{max} at the bottom of the NC clay layer.

To highlight the role of strain softening, Fig. 3 presents the results of two analyses with strain softening behavior in which the peak shear strength was kept unchanged up to shear strain of 5% and reduced linearly to 85% and 75% of the peak strength at shear strain of 15%. The larger displacements compared to the elastic-perfectly plastic results (also shown in the figure), clearly show the importance of strain softening on the earthquake response of slopes.

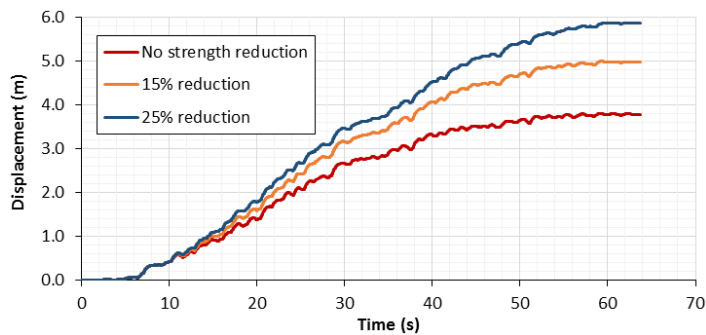


Fig. 3. Response of slope for different levels of strain softening

Taiebat and Kaynia (2010) have developed a simple and practical version of the plasticity model SANICLAY (Dafalias et al. 2006) that accounts for de-structuration (strain softening) and anisotropy, and have implemented it as a user-defined model in FLAC3D. In this model, the plastic potential surface in the triaxial p-q stress space is a rotated and distorted ellipse. The amount of rotation and distortion reflects the extent of anisotropy, and is controlled by an evolving variable α , which is scalar-valued in triaxial, and tensor-valued in multiaxial stress space. The model uses a non-associated flow rule that allows simulation of softening response under undrained compression following oedometric consolidation. Taiebat et al. (2011) used this model to compute 3-D earthquake response of a generic soft clay slope for different earthquake loading and material parameters. The results again highlight the important role of strain softening on the earthquake response of slopes.

3.2 Multi-Directional Shaking

Early research into multi-directional shaking was primarily concerned with liquefaction analyses for level ground conditions or stability of earth dams. Pyke et al. (1975) performed a number of multi-directional shaking table tests on clayey sand. They found that the total settlement caused by the two (simultaneous) horizontal ground motion components was the same as the sum of the settlements caused by the ground motion components applied separately. Stewart and Yee (2012) found similar results for a series of 1-D and 2-D simple shear tests on dune sand from a nuclear power plant in Japan. Seed et al. (1978) found the same was true for excess pore pressure generation in sands. In addition, Pyke et al (1975) noted that applying one horizontal and one vertical component increased the total settlement by 20 to 50% over the settlement caused by applying the horizontal component alone. Kammerer et al. (2003) performed extensive laboratory stress-controlled cyclic tests on granular soil and found that the soil response under multi-directional shearing tended to generate pore pressure faster than that of unidirectional shearing. Su and Li (2003) applied both unidirectional and multi-directional shaking to level saturated sand deposits in a centrifuge and found that the maximum pore pressure at great depths for multi-directional shaking was about 20% larger than in one-directional shaking and the difference reduced to about 10% near the surface.

Multi-directional shaking of slopes has more recently gained interest. Anantanavanich et al. (2012) performed seismic slope stability analyses for two generic offshore soft clay sites with depths of 20 m and 100 m and a slope angle of 10 degrees. They compared the estimated permanent displacements and excess pore pressures generated from applying one or both horizontal components of a ground motion at the same time. They found that multi-directional shaking predicted 20-40% increase in permanent displacements over unidirectional shaking. For the 100 m deep soil profile, multi-directional shaking predicted 30% increase in excess pore pressure at large depths, which reduced to 10% at the soil surface, whereas the 20

m deep soil profile predicted an increase in excess pore pressure between 20% and 40%.

Carlton and Kaynia (2016) conducted a number of numerical simulations in which 3-D slopes of NC clay with simple Mohr-Coulomb failure criterion were subjected to one-component and 3-component earthquake excitations. Through a number of case studies, they observed that inclusion of the earthquake component perpendicular to the slope direction increases the permanent downslope displacements and shear strains in the slope by 25%-50% and by 10%-50%, respectively. Figure 4 shows an example of the results for 3-component (above) and one-component (below) shaking. The shear strength increases linearly with depth with strengths of 5 kPa on surface and 300 kPa at depth 300 m. The slope angle is 15 degrees, and the earthquake record is the magnitude 6.5 California earthquake of 1954 at Ferndale City Hall scaled to 0.6 g on bedrock.

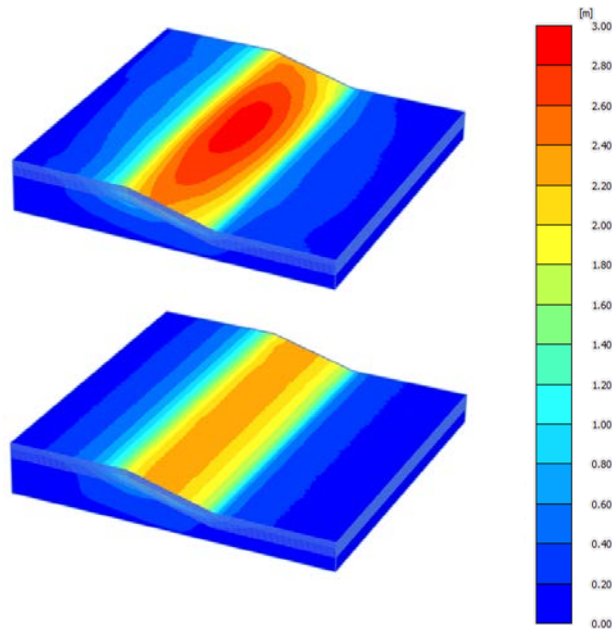
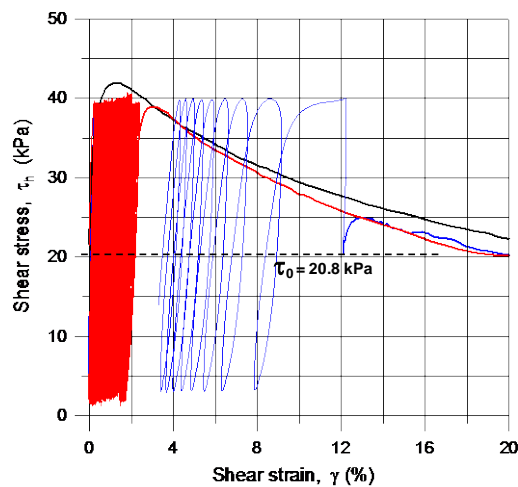


Fig. 4. Response of slope for 3-component (above) vs one-component (below) earthquake (adapted from Carlton & Kaynia, 2016)

The results of the analyses were also used to assess the accuracy of the displacement predictive equations by Bray and Travasarou (2007) and Kaynia and Saygili (2014). The former equation uses PGA on bedrock and the latter uses the peak acceleration on ground surface. The results showed that while the equation by Bray and Travasarou (2007) provided a good estimate of the displacements, the one by Kaynia and Saygili (2014) predicted lower values. The corresponding equations for permanent strains in Kaynia and Saygili (2014) gave generally larger values than

those simulated. The permanent shear strains are used to assess the static stability of slopes post earthquake loading. The mechanism is illustrated in Fig. 5 for cyclic shear tests on a sensitive clay in DSS (Andersen, 2009). The figure shows both the stress-strain curve under a monotonic static loading (black curve) and two static tests right after a number of cyclic loads (red and blue curves). The results show a significant reduction of the static shear strength after the cyclic loading. The reduction of the strength depends on the sensitivity of the clay and the accumulated shear strains during the cyclic loading, and varies with the type of clay, plasticity, consolidation stress and over-consolidation ratio, OCR.

Fig. 5. Direct simple shear test on normally consolidated sensitive clay showing effect of cyclic strain accumulation on post cyclic shear strength (after Andersen, 2009)



3.3 Three-Dimensional Geometry

Although three-dimensional numerical codes, such as PLAXIS and FLAC, have been available for some time, very few analyses of earthquake slope response with three-dimensional geometries have been reported in the literature. This could be attributed in part to the complexity of generating 3-D element meshes and demanding computational power, both of which have been extensively improved in recent years.

Another reason for ignoring 3-D effects is the findings from a number of studies on the static stability of slopes (e.g. Duncan, 1996) that have concluded that consideration of 3-D response improves the static safety factor. The studies reported in Azizian and Popescu (2006) for 3-D seismic analyses of submarine slopes have also concluded that the results of 2-D and 3-D analyses are generally close. The above studies have focused on the effect of 3-D model extension on the critical failure surface.

A different approach has been used by Ferrari (2012) to address the issue of 3-D slope response. Figure 6 shows a 3-D slope configuration with a homogeneous soil with $s_u = 25$ kPa and $G_{max} = 25$ MPa. In addition to the usual slope angle used in 2-D models in the x-direction, there is also a sloping face normal to the main direction (i.e. y-direction). The two slope angles are denoted as α and β in the following.

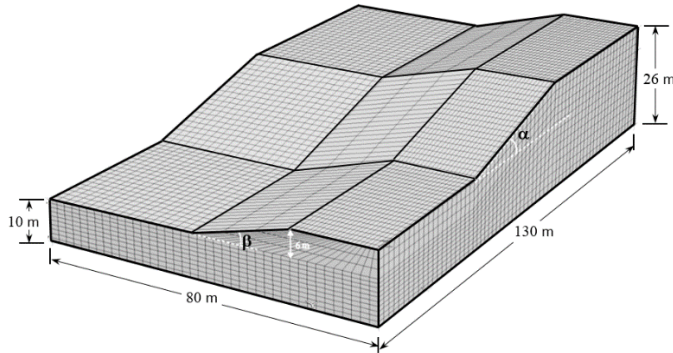


Fig. 6. Geometry and parameters of 3-D slope model

This model was excited by ten cycles of harmonic (sine) wave with different frequencies. Figure 7 displays contours of the computed permanent slope displacements for the case $\alpha = \beta = 1:4$, frequency of 2 Hz and peak acceleration equal to 0.15 g. Due to slope angle β , the static shear stresses in the soil elements in this model are larger than those in the corresponding 2-D models; this is expected to increase the nonlinear response of the soil and permanent displacements.

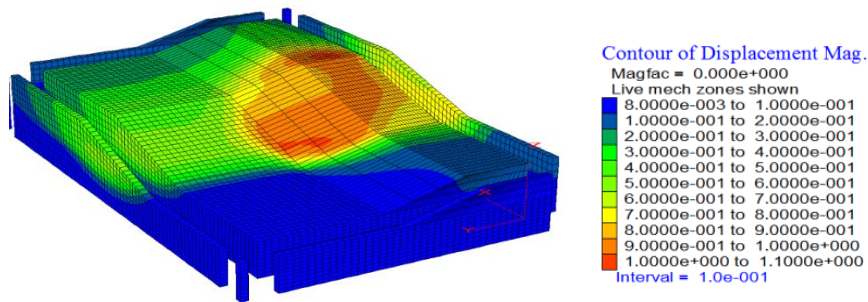


Fig. 7. Contours of permanent slope displacements for slope angles 1:4 and input peak acceleration 0.15 g

Figure 8 shows two cross-sections through the slope and normal to the direction of excitation. In order to assess the effect of 3-D geometry, the responses of these sections were evaluated separately as 2-D models under the same earthquake exci-

tation. Figure 9 displays the contours of earthquake induced displacements in section (a) together with the corresponding results in the same sections of the original 3-D model. Figure 10 shows the corresponding comparison for responses in section (b). Comparing the maximum displacements for these sections, one can observe that the additional slope normal to the main slope amplifies the displacements by a factor ranging from about 20% to 50%. These results point out to the importance of considering 3-D slope geometry in earthquake analyses.

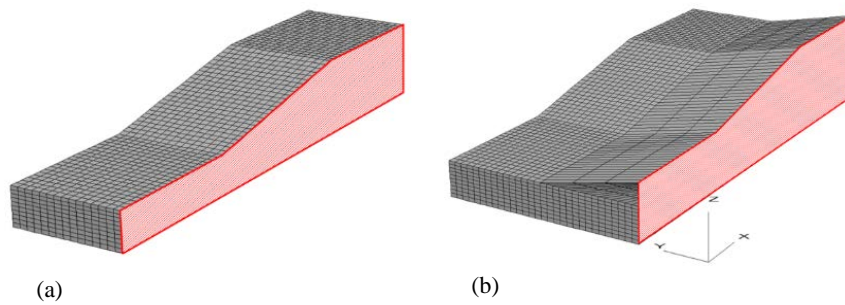


Fig. 8. Sections through 3-D slope and equivalent 2-D models

Fig. 9. Comparison between response of 3-D model at Section (a) in Fig. 8 with response of 2-D model (for color scale, see legend in Fig. 7)

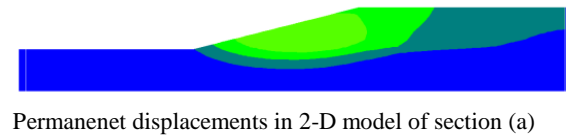
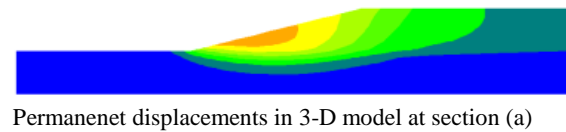
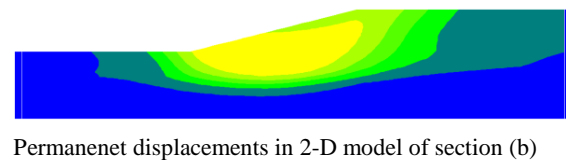
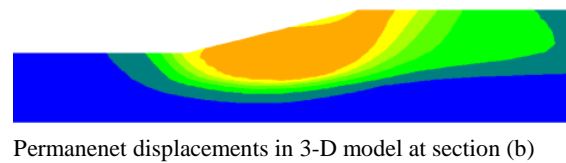


Fig. 10. Comparison between response of 3-D model at Section (b) in Fig. 8 with response of 2-D model (for color scale, see legend in Fig. 7)



4. Earthquake Response of Pipelines

Extensive research has been conducted on the static response of pipelines on soft seabed in the last decade (e.g. SAFEBUCK JIP). This is primarily due to increased oil and gas development in deep water where typically soft seabed is found. Observations and monitoring of the behavior of pipelines in these environments have unveiled challenging subjects related to the interaction between pipeline and seabed, such as buckling and the so-called pipeline walking. The SAFEBUCK JIP (e.g. White et al. 2011) has supported a program of research for tackling the uncertainties associated with the design of pipelines against lateral buckling and axial walking. During the pipe laying process, pipelines are subject to small amplitude vertical and horizontal oscillations, driven by the sea state and lay vessel motions. In the soft soils found in deep water, pipe embedment can exceed a pipe diameter, and this embedment has a significant effect on the lateral pipe–soil interaction and axial resistance (Westgate et al. 2013).

Research has also been carried out on the earthquake response of pipelines. Observed damages to pipelines in seismic events (e.g. O'Rourke and Liu 1999) have generally been attributed to two hazards: a) permanent ground deformation (PGD); and b) soil strain due to seismic wave propagation. Permanent ground deformation can be either localized and abrupt, as in fault rupture, or spatially distributed, such as in landslides and liquefaction-induced lateral spreading. Soil strains induced by seismic wave propagation are generally small (Younan, 2012). Depending on the pipe-soil coefficient of friction, the resulting pipeline strains can be equal to or less than ground strains in the case of a straight pipeline segment. However, it is possible that strain localizations may be induced by geometric discontinuities such as pipeline bends, tees and/or valves. One of the approaches for estimating the strains induced by seismic wave propagation is the ASCE approach (ASCE 1984, ASCE 2001) that is based on the assumption that a buried pipeline follows the ground motion. The maximum axial strain in the pipe can be approximated by the maximum ground strain, estimated as $\varepsilon = PGV/C$ where PGV is the peak ground velocity and C is the apparent wave propagation velocity.

Kaynia et al. (2014) have studied two key elements not covered by the above studies: a) earthquake response of pipelines on sloping seabed excited by asynchronous motions, and b) strain-softening behavior of soil along the pipeline. The following describes implementation of these features in a computational method.

Figure 1 shows an example of seabed topographic features that can be due to geological processes or earlier landslides. Due to the seabed topography and the long extension of the pipeline, points along the pipeline route experience different motions during an earthquake. These motions can be computed by 3-D models of the ground by a suitable software (e.g. FLAC3D and PLAXIS3D). Alternatively, if the pipeline does not have extensive bends out of plane, one can model only 2-D section of the ground along the pipeline using a 2-D software. The numerical model,

QUIVER-pipe (Kaynia, 2012b) addresses both the asynchronous earthquake motions and the strain-softening soil behavior at the soil-pipe interface (Kaynia et al., 2014).

Figure 11 illustrates an idealization of pipe-soil interaction in a pipeline under earthquake loading. The pipeline has an arbitrary geometry (for simplicity only a 2-D geometry is shown in Fig. 11) and is placed on a number of springs representing pipe-soil interaction. The springs are excited at their bases by different acceleration time histories computed by appropriate 2-D/3-D numerical tools. A common practice in pipeline analysis is to ignore the pipeline mass and apply the earthquake motion as static displacements under the springs. While the submerged weight of pipes is often small, the total weight, which steers the dynamic response through inertia forces, could be quite large compared to the soil resistance against pipe movement. Ignoring the mass of the pipe might thus result in un-conservative conditions. This has been illustrated by an analysis in Kaynia et al. (2014). Moreover, by treating the earthquake excitation statically, one cannot capture the out-of-phase movements, which could lead to larger differential soil movements along the pipeline. This effect could also lead to un-conservative results.

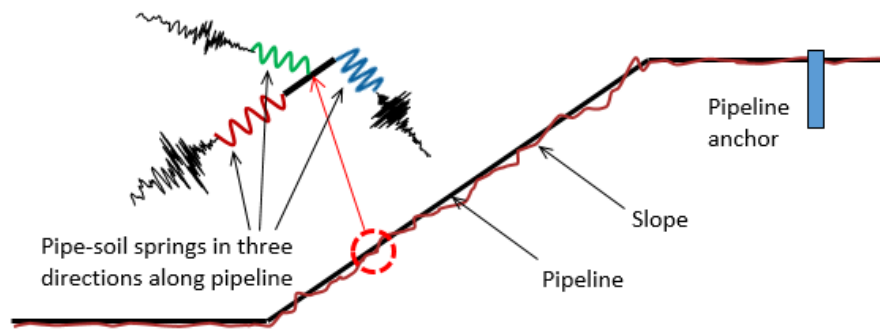


Fig. 11. Pipe-soil interaction model for analysis of response due to asynchronous earthquake motions in three directions

The soil springs in *QUIVER-pipe* are specified along the pipeline (axial springs) and perpendicular to its axis (lateral springs). The pipeline can be laid freely on the ground surface and might additionally be anchored at a point on the ground surface on top of the slope, as shown in Fig. 11. The anchor has the function of resisting the axial load resulting from the tendency of the pipe to 'walk' down the slope. In practice, the anchor is installed such that the connection has a slack length (typically in the range 200-300 mm).

The pipe-soil interaction in *QUIVER-pipe* is represented by strain-softening springs with either concave or convex forms exemplified in Fig. 12. These springs are distributed in the three directions along the pipeline. The developed model is based on the finite element method consisting of 3-D beam elements and distributed

soil springs along the pipe in the three directions. The pipe masses and the distributed springs are lumped at the nodes. The main source of damping after reaching the peak strength is energy dissipation through the hysteretic nonlinear response in the springs that follows Masing's rule (Masing, 1926). The model is excited by three independent acceleration time histories under the soil springs at each node. A model with N nodes contains $6N$ degrees of freedom corresponding to the six degrees of freedom at each node.

Fig. 12. Strain softening springs for pipe-soil interaction

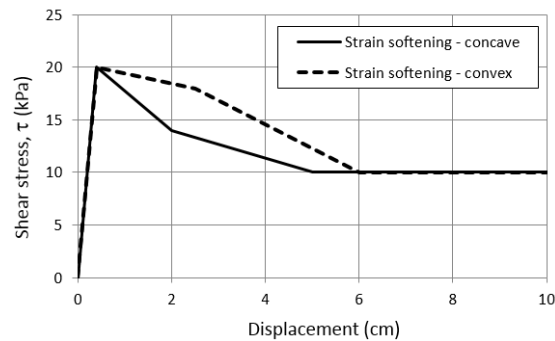


Figure 13 presents an example of results from an earthquake pipe-soil interaction analysis. See Kaynia et al. (2014) for details of the soil and pipe model and earthquake excitation. Figure 13a shows the FE mesh, and Fig. 13b displays the maximum earthquake-induced axial forces computed along the pipeline. It should be noted that the forces are plotted in absolute value; moreover, they are not simultaneous. The maximum permanent displacement on the slope surface is about 2 m. As expected, the axial force reaches a peak value close to the top of the slope.

Figure 13c presents the variation of the corresponding maximum bending moments along the pipeline. As opposed to the axial force, the bending moment displays a very sharp increase at top of the slope. These results are physically justifiable in view of the remarkable gradient of the displacements around this location.

5. Response of Seabed Facilities

Due to recent trends in the offshore industry to move to deeper water, most of the operations related to oil and gas production and processing are being carried out close to the wells. This requires installation of different facilities and structures directly on the seabed and connecting them by pipelines, jumpers and spools. These installations vary in size from wellhead trees (albeit relatively heavy) to heavy manifolds and templates. Templates are often large steel structures used to support or protect manifolds. Manifolds vastly vary in shape, size and function, and could reach as high as 30 m in height and even larger in plan dimensions.

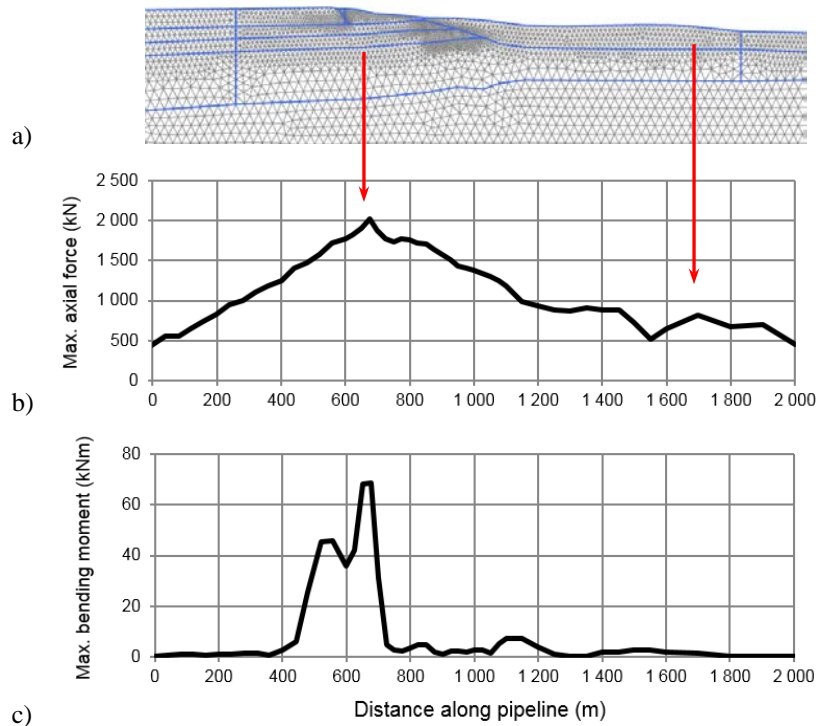


Fig. 13. Absolute values of maximum pipe forces along pipeline: a) FEM mesh of slope – pipeline lies on top surface, b) axial force, c) bending moment

Depending on soil conditions and available installation technique and schedule, manifolds could be founded on several (typically 4) piles, on large single bucket foundations, or on steel mudmats. The piles/buckets are often installed by base suction, while mudmats are placed directly on the seabed with skirts penetrating into the seabed to provide additional lateral resistance. The design of these foundations are often driven by size requirements and for loads rather than by weight. Therefore, they end up being quite stiff for the mass they carry which results in relatively high natural frequencies, typically in the range 3-5 Hz.

The large natural frequencies represent some challenges in the dynamic and earthquake analyses of the foundations, including handling of added soil mass and damping. Designers often ignore these parameters or assign arbitrary values without any rigorous analyses. For large foundations, high natural frequency corresponds to large radiation damping that could be translated to damping ratios as high as 100%. The radiation damping, which is often ignored in design, would considerably reduce the earthquake-induced accelerations (and loads on the manifold and foundation).

In order to highlight the importance of rigorous modelling, three realistic foundations were considered in a realistic soft soil profile representative of deep water locations. The three designs and their key parameters are (Kaynia and Wang, 2017):

- a) 4-pile foundation: Diameter, length and wall thickness, $D = 3$ m, $L = 12$ m, $t = 15$ mm, center spacing of piles 9 m
- b) Bucket foundation: $D = 8$ m, $L = 9$ m, $t = 25$ mm
- c) Mudmat: Plan dimensions and length, $17 \text{ m} \times 17 \text{ m} \times 1.0$ m.

The soil profile considered in the analyses represents a realistic soft soil site with approximately a linear variation of shear strength with depth. The strain-compatible shear modulus, that is, after consideration of reduction due to shear strains induced by a strong earthquake, varies from approximately 2 MPa on the seabed to 75 MPa at 100 m depth. The mass density of the soil is relatively constant with depth, except for the 2 m soil below the seabed, and is equal to 1580 kg/m^3 . The template mass is 500 tons.

Computation of the pile-group impedances was carried out by PILES (Kaynia, 1982). The impedances of the bucket foundation were computed using the FE solution by Tassoulas (1981), and the impedances of the mudmat were computed by the Green's function-based solution of Kaynia et al. (1998). All these methods are rigorous tools based on analytical solutions of wave propagation in layered media and perfectly handling of infinite boundaries. The methods work in the frequency domain and result in impedances as complex quantities with the real parts reflecting the combined effect of foundation stiffness and added soil mass, and the imaginary part reflecting the hysteretic and radiation damping. The imaginary part was used in this paper to compute the equivalent damping ratio of the foundations.

Figure 14 plots the real and imaginary parts of the computed vertical impedances of the three foundations as functions of frequency. The three foundations were slightly modified to give about the same vertical static stiffness (at $f = 0.0$ Hz) equal to about 7 MN/m.

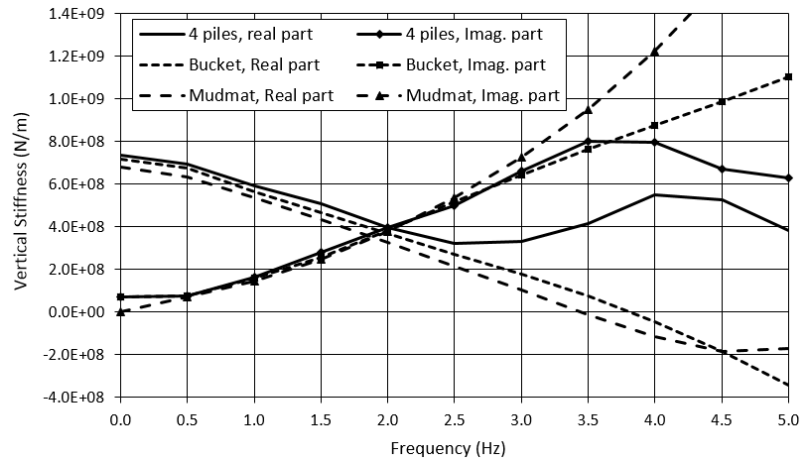
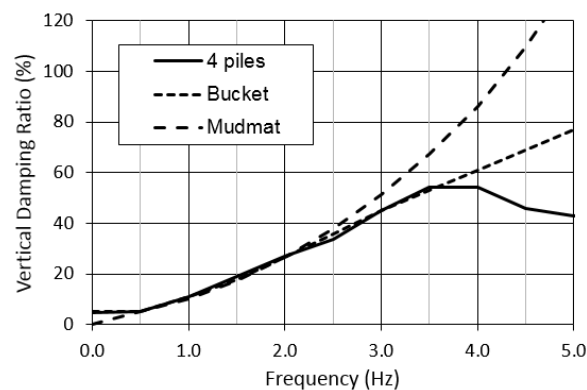


Fig. 14. Dynamic impedances of three foundation types studies in this paper: i) 4-pile group, ii) Bucket foundation, iii) Mudmat.

It is interesting to note that, although the three foundations have the same static stiffness, their dynamic stiffnesses (real part) are quite different. While the dynamic stiffness of the pile group shows relatively moderate variation with frequency, indicating a small added soil mass, the dynamic stiffnesses of the bucket foundation and mudmat are strongly frequency-dependent, representing a large added soil mass. For example, using the parabolic form of the stiffness of the bucket foundation, one could compute an equivalent added mass of about 1200 tons. This is more than double the manifold mass and almost double the mass of the soil plug (700 tons). Despite this fact, most engineers assume the added soil mass equal to the soil plug mass. Using the added soil mass and the mass of the manifold (500 tons), one could compute a natural frequency of vertical vibration equal to 3.3 Hz.

Figure 15 plots the variation of the computed foundation damping for the above foundation designs. The figure shows that the three designs have fairly similar damping values. For the computed natural frequency of 3.3 Hz, one gets a damping ratio of about 50%. As stated earlier, this damping is so large that it prohibits the foundation from oscillation and consequently reduces the vertical earthquake load dramatically.

Fig. 15. Damping ratio as function of frequency for three foundation types studied above: i) 4-pile group, ii) Bucket foundation, iii) Mudmat.



While damping can dramatically reduce the earthquake loads on subsea structures, its impact on a system of assembled subsea facilities could be even more significant. Manifolds and other installations, such as PLEM and PLETs, are often connected by elements such as spools that lie on the seabed between the facilities. These elements are relatively light and flexible and follow the motions of the facilities at the two ends. Large earthquake displacements in the structures could result in overstress in these elements at the contact points and the point of touching the ground. A realistic, lower displacement of the seabed installations could thus have a major design implication for these sensitive elements.

Another topic in this discussion is the effect of water on the earthquake response of seabed foundations. The study by Kaynia et al. (1998) has shown that water can practically be ignored in the horizontal and rocking responses of seabed founda-

tions. However, the effect is relatively large in the vertical direction at higher frequencies, especially in the form of added mass. Figure 16 displays the effect of different water depth on the vertical impedance of the mudmat studies above. The results are in agreement with those in Kaynia et al. (1998) which show that water has an effect only up to a depth of the order of the foundation dimensions.

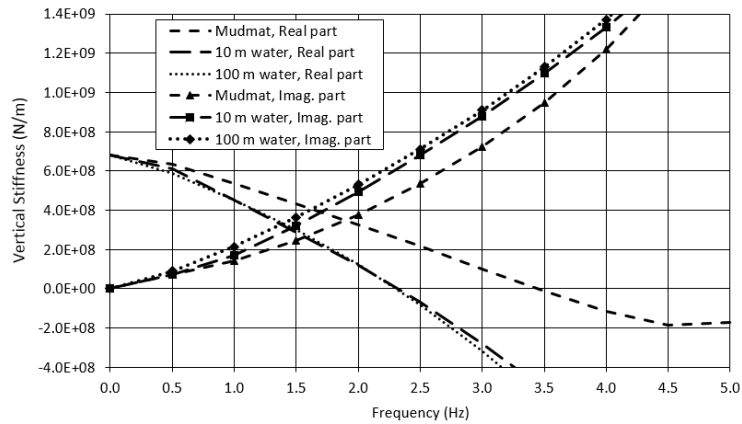


Fig. 16. Dynamic impedances of mudmat foundation for different water depth including results for case of no water for comparison

6. Response of Platforms

Earthquake analysis of fixed platforms follow the standard models used in traditional soil-structure interaction (SSI) analyses. Therefore, two approaches are utilized: a) one-step solutions based on integrated models of soil and structure, and b) sub-structuring solutions where the soil and structure domains are modelled and analyzed as separated domains (Kausel, 2012). One of the commonly used sub-structuring methods is the well-known three-step solution (Kausel et al, 1978) which was developed for cases with rigid foundations. In this method, the analysis is divided into the three steps, namely, *kinematic interaction*, *impedance calculation* and *inertial interaction*. While it is ideal to perform earthquake analyses by the one-step method, there are several obstacles for its use in practice. The first obstacle is that structural designers rarely use the required state-of-the-art SSI softwares, for example SASSI (Lysmer et al., 1981). The second issue is that engineering usually involves several EPC contractors, each with their own sets of tools and procedures that make compatibility between the analyses a challenge for the project. Therefore, despite its limitations, the three-step methods as described in the following, is the preferred approach in most SSI analyses.

6.1. Jacket Structures on Piles

Offshore jackets are made of tubular steel members, and are usually piled into the seabed. The earthquake analysis of these types of platforms are commonly based on a special version of the three-step method in which the piles are included in the structural model and the interaction with the soil is accounted for by the use of non-linear pile-soil springs commonly known as p-y, t-z and Q-z springs. The p-y curves, in which p denotes the lateral soil reaction per unit length of the pile and y denotes the lateral deflection, have evolved from research in the oil and gas industry during the 1970s. The research has been based on tests using 324 mm diameter steel-pipe piles in soft clay by Matlock (1970), 610 mm diameter steel-pipe piles in stiff clays by Reese et al. (1975), 914 mm diameter RC drilled piles in stiff clays by Reese and Welch (1975), and 619 mm diameter steel-pipe piles in sands by Cox et al. (1974). The p-y curves established from these studies led to recommendations in the American Petroleum Institute standards for oil and gas installations (API, 1993). These curves were established with special focus on storm loading which is often the dominating environmental load on jacketed structures. Because the dominant period of storm load is typically 10 seconds, the p-y curves have been defined with low initial stiffness to ensure higher SSI natural periods that would represent more conservative conditions. Recognizing the importance of capturing the stiffer response for other loads, especially earthquake, the latest version of API (2011) has increased the initial stiffness of the p-y curves. Moreover, considering that the initial pile load tests were performed on smaller diameter piles (for example 0.61 m in Reese et al, 1974), attempts have been made to modify the p-y curves for the effect of pile diameter and stiffer initial stiffness of the piles (e.g., Stevens and Audibert, 1979 and Jeanjean, 2009). Other issues in connection with earthquake loading relate to 1) modeling of cycling response using p-y curves, 2) incorporation of radiation damping at higher frequencies, and 3) consideration of liquefaction. These are briefly discussed in the following.

The centrifuge experiments by Boulanger et al. (1999) were used to verify a model based on cyclic p-y curves. To this end, a nonlinear p-y element was developed based on the results of Matlock (1970) in which the nonlinear p-y spring is replaced by three springs representing elastic, plastic and gap components in series. The radiation damping was then added in parallel to the elastic spring representing the far-field response. The p-y spring set at each depth is excited by the earthquake motion in the free field computed from site response analyses at that depth. The radiation damping could be estimated by simple models (e.g. Gazetas, 1991). In cases that the earthquake loading is not very strong so that the response can be captured by an equivalent linear method, one can resort to the standard three-step method in which the piles are represented by their dynamic impedances at their pile head. Rigorous numerical tools (e.g. Kaynia, 1982) or simple solutions (e.g. Dobry and Gazetas, 1988) could be used for the computation of pile impedances that can be converted to equivalent stiffness-mass-damping elements.

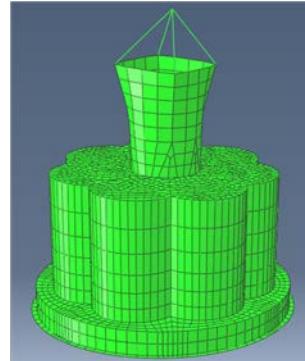
Incorporation of liquefaction in analysis of piles is a complex and uncertain issue that is still under research. The uncertainty is primarily due to the complexity of liquefaction and its quantification. Dash et al. (2008) made a summary of practical solutions used for capturing behavior of piles in liquefiable soil. The solutions include those that completely ignore soil resistance during liquefaction (as proposed in some design codes) and those methods that reduce the strength of p-y curves for (non-liquefied) sands. Among the latter approach, one could find the well-known p-multiplier method based on SPT data and the Cu-factor method proposed by Liu and Dobry (1975) based on centrifuge test data that assumes a strength degradation factor, $C_u = 1 - r_u$, where r_u is the excess pore pressure ratio. Alternatively, one could compute friction angle corresponding to the residual shear strength (e.g. Boulanger and Idriss, 2016) and use it to define p-y curves. Some experimental results have shown different forms in the shape of p-y curves. For example, the full-scale tests by Rollins et al. (2005) on single piles and pile groups subjected to blast induced liquefaction and back-calculation of the data have shown that the p-y curves from the test results display a concave pattern at full liquefaction. It should be noted that while the condition of liquefaction often represents a more critical (conservative) case for the pile design, it might create a more favorable case for design of the platform. Therefore, in such cases, one should also analyze the platform assuming that the soil would not liquefy.

6.2. Gravity Based Structures

Earthquake analysis of gravity-based structures (GBS) is commonly performed by the three-step method. The conventional three-step method is based on the assumption of rigid foundation and linear soil response. Younan et al. (2015) presented a benchmark three-step earthquake analysis of a concrete GBS with an apparently stiff foundation caisson. The objective of the benchmark study was to assess the accuracy of the three-step method by comparing the results of a one-step integrated analysis with those of the three-step method in which the frequency-dependent complex impedances of the foundation are converted into real-valued sets of spring-mass-dashpot elements, so-called lumped parameter foundation model, LPFM. The procedure often used in practice for calculating the parameters of LPFM is as follows: 1) compute the static stiffness, K_{st} , and added soil mass, M , by fitting a parabola in the form $K_{st} - M \cdot \omega^2$ to the real part of the foundation impedance (ω is frequency in rad/s), 2) compute the damping constant, C , from the imaginary part of the foundation impedance by fitting a line in the form $C \cdot \omega$ to the imaginary part of the impedance.

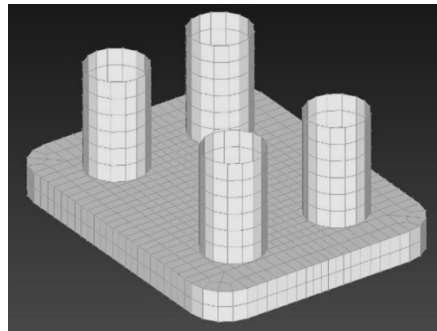
Figure 17 illustrates the finite element model of the GBS caisson used in SASSI (Lysmer et al. 1981). A number of points were selected on the model for computing the response spectra by the two methods. The comparison was successful indicating that the assumption of rigid base was satisfactory for the earthquake analysis of this structure (Younan et al. 2015).

Fig. 17. Finite element model of example concrete GBS



In cases of flexible bases, one needs to develop distributed LPFM that would give foundation impedance parameters at predefined nodes or per square meter of the base. As an example, Fig. 18 shows the FE model of a concrete GBS with approximate base dimensions 110 m by 130 m. In view of the relatively low height of the caisson, this GBS cannot accurately be modelled as rigid. The distribution of the impedance parameters, namely stiffness, added soil mass and damping, is not unique and depends on the details of the structure and the mode of response, that is, horizontal or vertical. For this purpose, one should establish the parameters by accounting for the loading together with the foundation and structural details.

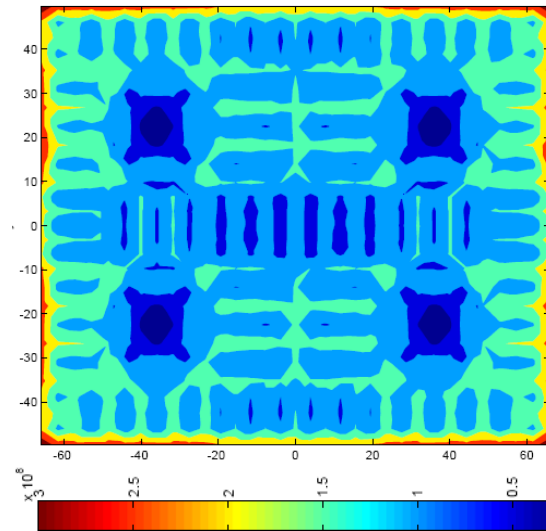
Fig. 18. Finite element model of base and shafts in a large concrete GBS with approximate base dimensions 100 m by 130 m



One of the practical solutions developed for this purpose is due to Tabatabaie and Ballard (2006). The solution consists of the following steps: a) perform a one-step SSI analysis of soil-structure in the frequency domain for a given earthquake excitation (for example horizontal or vertical) using a coarse model of the foundation and structure, b) compute the complex-valued forces and corresponding displacements at the nodes of the base, c) divide the forces and displacements and compute the complex impedances at the nodes, and derive the parameters of LPFM at the nodes following the procedure described above for rigid foundations. The distributed LPFM computed by this procedure can then be used in an SSI model of the structure with refined mesh as required for the detailed design. Figure 19 display an example of this type of computation for the distributed vertical spring values for

the GBS platform shown in Fig. 18 for vertical earthquake loading. The results in Fig. 19 show that the stiffness is lowest where the foundation is stiffest (for example under the shafts and internal stiffeners in the GBS caisson) and are largest outside, and close to the edges.

Fig. 19. Distribution of vertical springs over base of GBS shown in Fig. 16 for vertical earthquake loading

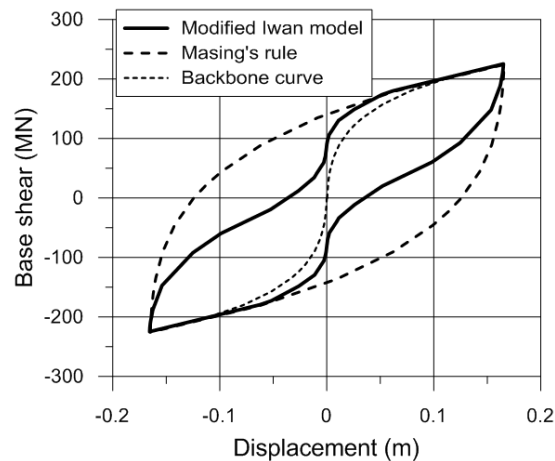


Medium to large earthquake shaking induce larger inertial loads in the platform causing nonlinear soil response and permanent lateral displacement of the platform. In such cases, a performance-based design in which the soil-structure interaction is handled by using nonlinear force-displacement relationships at soil-foundation interface (so-called backbone curves) can provide a realistic picture of the earthquake response and an economical solution. A major challenge in this type of analyses is accurate representation of damping in the nonlinear cyclic response by the backbone curves, often referred to as hysteretic damping. Most available models represent the backbone curves with the help of Masing's rule which is a kinematic hardening model easily represented by a series of parallel elasto-perfectly plastic spring first proposed by Iwan (1967). Figure 20 shows an example of the nonlinear hysteretic response (dashed line) in a horizontal foundation spring of a platform following Iwan's model. The amount of hysteretic damping, which is directly related to the area circumscribed in a closed response loop, is about 33% that is a large value for this displacement.

Different solutions have been proposed for limiting the foundation hysteretic damping. One of these solutions, which has been implemented and verified against actual measurements of Troll Platform (Kaynia et al. 2015), is based on modifying the curvature of the backbone curve (Kaynia and Andersen, 2014). Another solution that has been tried by Younan et al. (2015) in the nonlinear SSI analysis of Hebron GBS is to deviate from the Masing's rule by defining different unloading rules that would result in slimmer hysteresis loops. A simple way to achieve this is through a

modified Iwan's mechanical model in which a selected number of the elastic-plastic springs are replaced by corresponding nonlinear elastic springs. The resulting model will reproduce follow same backbone curve but with a pinched hysteretic response. This is shown in Fig. 20 (solid line). For the curve shown in this figure, the damping ratio is reduced to 19% by this modification. The figure also plots the backbone curve (dotted line) for reference.

Fig. 20. Nonlinear hysteretic response following Masing's rule (dashed line) and modified Iwan model (solid line) for given backbone curve (dotted line).



7. Summary and Conclusions

This paper presented a number of geotechnical issues encountered in earthquake design of offshore structures and subsea facilities. The paper addressed some of the more recent approaches and solutions in geotechnical earthquake design of both shallow water and deep-water structures and facilities such as platforms with large bases, pipelines traversing slopes and seabed installations. It was demonstrated how incorporation of radiation damping and nonlinear soil-structure interaction in offshore installations could optimize the design. It was also highlighted how consideration of several factors such as strain softening and three-dimensional shaking that are often ignored in design, could affect the response of submarine slopes and pipelines. Finally, various solutions for earthquake SSI analyses of platforms were reviewed, and solutions were proposed for realistic representation of the foundation nonlinear response including hysteretic damping.

Acknowledgment

The author would like to acknowledge partial support from the project "Reducing cost of offshore wind by integrated structural and geotechnical design (REDWIN)" funded by the Norwegian Research Council, grant number 243984.

8. References

- American Petroleum Institute (API) (1993). Recommended practice for planning, designing, and constructing fixed offshore platforms – Working stress design. API RP2A-WSD, 20th Ed., Washington D.C.
- American Petroleum Institute (API) and International Organization for Standardization (ISO), (2011), ANSI/API Specification RP 2GEO. Geotechnical and Foundation Design Considerations for Offshore Structures. API, Washington, DC.
- Anantanavanich T., Pestana J., Carlton B. (2012). Multidirectional site response analysis of submarine slopes using the constitutive model MSimpleDSS. *Proc. 15th World Conf. on Earthquake Engineering*, Lisbon, Portugal, 24-28 September.
- Andersen, K.H. (2009). Bearing capacity of structures under cyclic loading; offshore, along the coast and on land. *Can. Geotech. J.* 46: 513-535.
- ASCE (1984). Guidelines for the Seismic Design of Oil and Gas Pipeline Systems, Committee on Gas and Liquid Fuel Lifelines.
- ASCE (2001). Guidelines for the Design of Buried Steel Pipe, American Lifelines Alliance.
- Azizian, A, and Popescu, R (2006). Three-dimensional seismic analysis of submarine slopes. *Soil Dynamics and Earthquake Eng.*, 26, 870–887.
- Bray, J.D., and Travasarou, T. (2007). Simplified procedure for estimating earthquake-induced deviatoric slope displacements. *Journal of Geotechnical and Geoenvironmental Engineering*, ASCE 133(4): 381–392.
- Boulanger, R., Curras, C., Kutter, B., Wilson, D. and Abghari, A. (1999). Seismic soil-pile-structure interaction experiments and analyses. *J. Geotech. Geoenviron. Eng.*, vol. 125:9, 750-759.
- Boulanger RW, Idriss IM. (2016). CPT-based liquefaction triggering procedure. *J Geotech Geoenviron Eng*, ASCE; 142(2): 04015065.
- Carlton, B.D. and Kaynia, A.M. (2016). Comparison of the Seismic Response of Offshore Slopes Using 1, 2, or 3 Ground Motion Components. Paper OTC-26961, Proc. Offshore Technology Conference, Houston, Texas, 2-5 May.
- Cox, W.R., Reese, L.C., and Grubbs, B.R. (1974). Field testing of laterally loaded piles in sand. *Proc. 6th Offshore Technology Conference*, Houston, 459–472.
- Dafalias, Y.F., Manzari, M.T. and Papadimitriou, A.G. (2006). SANICLAY: simple anisotropic clay plasticity model. *Numerical and Analytical Methods in Geomechanics*, 30 (12), 1231–1257.
- Dash, S.R., Bhattacharya, S., Blakeborough, A. and Hyodo, M. (2008). P-y curve to model lateral response of pile foundations in liquefied soils. *Proc. 14th World Conf. on Earthquake Eng.*, Oct 12-17, 2008, Beijing, China.
- Dobry R. and Gazetas, G. (1988). Simple method for dynamic stiffness and damping of floating pile groups. *Geotechnique*, 38(4), 557–574.
- Duncan, J. M. (1996). State-of-the-art: limit equilibrium and finite element analysis of slopes. *ASCE Journal of Geotechnical and Geoenvironmental Eng.*, 122 (7), pp 577–96.
- Ferrari, G. (2012). Three-dimensional earthquake response of slopes. MSc thesis, Dept. of Civil Eng., University of Bologna and Norwegian Geotechnical Institute.
- Gazetas, G. (1991). Foundation Vibrations. in: *Foundation Engineering Handbook*, (H.Y. Fang, ed.), Van Nostrand Reinhold, New York, NY, 553-593.
- ISO 19901-2:2004, (2004). Petroleum and natural gas industries - Specific requirements for offshore structures - Part 2: Seismic design procedures and criteria.
- Itasca Consulting Group, Inc., FLAC3D - Fast Lagrangian Analysis of Continua in 3 Dimensions”, Minneapolis, Minnesota.
- Iwan WD. (1967). On a class of models for the yielding behavior of continuous and composite systems. *Journal of Applied Mechanics*. 34(3):612–617
- Jeanjean, P. (2009). Re-assessment of p-y curves for soft clays from centrifuge testing and finite element modelling. *Proc. Offshore Technology Conference*, paper OTC 20158.

- Kammerer, A., Pestana, J., and Seed, R. (2003). Behavior of monterey 0/30 sand under multidirectional loading conditions. *Geomechanics: Testing, Modeling, and Simulation*, Geotechnical Special Publication 143.
- Kausel, E. (2010). Early history of soil–structure interaction. *Soil Dynamics and Earthquake Engineering*, 30, 822–832
- Kausel, E., Whitman, R.V., Morray, J.P. and Elsabee, F. (1978). The spring method for embedded foundations. *Nuclear Engineering and Design*, Vol. 48, pp. 377-392.
- Kaynia, A.M. (1982). Dynamic stiffness and seismic response of pile groups. Research report R82-03, Dept. of Civil Engineering, MIT, Cambridge, USA.
- Kaynia, A.M. (2017). Earthquake response of offshore wind turbines. Invited Theme Lecture. *Proc. 3rd Int. Conf. Performance Based Design in Earthquake Geotechnical Eng.*, PBD III. Vancouver, Canada. July 16-19.
- Kaynia, A.M. and Wang, L.Z. (2017). Seismic response of subsea facilities. *Proc. Int. Symp. Coastal and Offshore Geotechnics, ISCOG 2017*, Hangzhou, China, 5-7 July, pp. 25-27.
- Kaynia, A.M. (2012a). *QUIVER_slope – numerical code for one-dimensional seismic response of slopes with strain softening behavior*. NGI Report 20071851-00-79-R, 8 June 2012.
- Kaynia, A.M. (2012b). *QUIVER_pipe: Numerical code for nonlinear seismic analysis of pipeline-soil interaction*. NGI Report 20071851-00-83-R, 8 June 2012.
- Kaynia, A.M., Kausel, E., and Madshus, C.M. (1998). Impedances of Underwater Rigid Square Foundations. *Proc. ASCE Spec. Conf. Geotech. Earthquake Engng*, Seattle, WA, USA, 1283–1293.
- Kaynia, A.M., Dimmock, P. and Senders, M. (2014). Earthquake response of pipelines on submarine slopes. *Proc. Offshore Technology Conference*, Paper OTC-25186, Houston, Texas, 5-8 May.
- Kaynia, A.M. and Saygili, G. (2014). Predictive models for earthquake response of clay and sensitive clay slopes. Chapter 18 in *Perspectives on European Earthquake Engineering and Seismology*, (A. Ansal, Ed.), Springer, New York, 557-584.
- Kaynia, A.M. and Andersen, K.H (2015). Development of nonlinear foundation springs for dynamic analysis of platforms. *Proc. Frontiers in Offshore Geotechnics III*, ISFOG, (V. Meyer, Ed.). Taylor & Francis Group, London, ISBN: 978-1-138-02848-7, pp. 1067-1072.
- Kaynia, A.M., Norén-Cosgriff, K., Andersen, K.H. and Tuen, K.A. (2015). Nonlinear foundation spring and calibration using measured dynamic response of structure. *Proc. ASME 2015 34th Int. Conf. on Ocean, Offshore and Arctic Engng, OMAE2015*, paper OMAE2015-41236. May 31-June 5, St. John's, Newfoundland, Canada.
- Lysmer, J., Tabatabaie-Raissi, M., Tajirian, F., Vahdani, S. and Ostadan, F. (1981). SASSI – A System for Analysis of Soil-Structure Interaction. *Report UCB/GT 81-02*, University of California, Berkeley, USA.
- Masing, G. (1926). Eigenspannungen und Verfestigung beim Messing. *Proc. 2nd Int. Congress on Applied Mechanics*, Zurich. pp. 332–335.
- Matlock, H. (1970). Correlations for design of laterally loaded piles in soft clay. *Proc. 2nd Annual Offshore Technology Conference*, 577–594.
- Nadim, F., Biscontin, G. and Kaynia, A.M. (2007). Seismic triggering of submarine slides. *Proc. Offshore technology Conference*, Paper 18911, Houston, Texas, April 30 – May 3, 2007.
- O'Rourke, M.J. and Liu, X. (1999). Response of Buried Pipelines Subject to Earthquake Effects. MCEER Monograph # 3, University at Buffalo, New York.
- Park, D.S. and Kutter, B.L. (2015). "Static and seismic stability of sensitive clay slopes", *Soil Dynamics and Earthquake Engineering*, 79, 118–129.
- PLAXIS 3D, (2015), PLAXIS, Delft, The Netherlands.
- Pyke, R.M., Seed, H.B., and Chan, C.K. (1975). Settlement of sands under multidirectional shaking. *Journal of Geotechnical Eng. Div.*, ASCE, 101(GT4): 379-398.
- Reese, L., Cox, W. and Koop, F. (1975). Field testing and analysis of laterally loaded piles in stiff clay. *Proc. 7th Offshore Technology Conference*, Houston, 671–690.
- Reese, L.C. and Welch, R. (1975). Lateral loading of deep foundations in stiff clay. *J. Geotech. Engrg. Div.*, 101(7), 633–649.

- Rollins, K.M., Gerber, T.M., Lane, J.D. and Ashford, S. (2005). Lateral resistance of a full-scale pile group in liquefied sand. *Journal of Geotechnical and Geoenv. Eng., ASCE*, 131 (1): 115–125.
- Seed, H.B., Pyke, R.M., and Martin, G.R. (1978). Effect of multi-directional shaking on pore-pressure development in sands. *Journal of Geotechnical Eng. Div., ASCE*, 104(GT1): 27-44.
- Stevens, J.B., and Audibert, J.M.E. (1979). Re-examination of the p-y curve formulations. *Proc. 11th Offshore Technology Conference*, Houston, 397–403.
- Stewart, J.P., and Yee, E. (2012). Nonlinear site response and seismic compression at vertical array strongly shaken by 2007 Niigata-ken Chuetsu-oki Earthquake. Report, National Earthquake Hazards Reduction Program, Reston, VA.
- Su, D. and Li, X. (2003). Centrifuge tests on earthquake response of sand deposit subjected to multi-directional shaking. *Proc. 16th ASCE Engineering Mechanics Conference*, University of Washington, Seattle.
- Tabatabaie, M. and Ballard, T. (2006). Distributed parameter foundation impedance model for time domain SSI analysis. *Proc. 8th US National Conference on Earthquake Eng. commemorating 100th anniversary of the 1906 San Francisco Earthquake*, San Francisco.
- Taiebat, M. and Kaynia, A.M (2010). A practical model for advanced nonlinear analysis of earthquake effects in clay slopes. Paper No. 1.09a, *Proc. Recent Advances in Geotechnical Earthquake Eng. and Soil Dyn.*, San Diego, California, 24-29 May.
- Taiebat, M., Kaynia, A. M., and Dafalias, Y. F. (2011). Application of an anisotropic constitutive model for structured clay to seismic slope stability. *Journal of Geotechnical and Geo-environmental Engineering*, ASCE, 137, No. 5, 492-504.
- Tassoulas, J.L. (1981). Elements for numerical analysis of wave motion in layered media. Research report R81-12, Dept. of Civil Engineering, MIT, Cambridge, USA.
- Westgate, Z.J., White, D.J. and Randolph, M.F. (2013). Modelling the embedment process during offshore pipe-laying on fine-grained soils. *Can. Geotech. Journal*. 50: 15–27.
- White, D.J., Ganesan, S.A., Bolton, M.D., Bruton, D.A.S., Ballard, J.C. and Langford, T.E. (2011). SAFEBUCK JIP – Observations of axial pipe-soil interaction from testing on soft natural clays. *Proc. Offshore Technology Conference*, paper OTC 21249. 2-5 May 2011, Houston, Texas, USA.
- Younan, A.H. (2012). Simulating seismic wave motions for pipeline design. *Proc. Twenty-second Int. Offshore and Polar Engineering Conference, ISOPE*. Rhodes, Greece, June 17–22, 2012.
- Younan, A.H., Kaynia, A.M., Loo, M.M., Widiyanto and Khalifa, J. (2015). Seismic design of Hebron platform - an integrated soil-structure-interaction approach. *Proc. ASME 2015 34th Int. Conf. on Ocean, Offshore and Arctic Engng, OMAE2015*, paper OMAE2015-42134. May 31-June 5, St. John's, Newfoundland, Canada.